Distinct roles of M1 and M3 muscarinic acetylcholine receptors controlling oscillatory and non-oscillatory $[Ca^{2+}]_i$ increase

Kyoko Nakamura[a], Kozo Hamada[b,c], Akiko Terauchi[b,c], Minoru Matsui[d], Takeshi Nakamura[a,b], Takao Okada[a] and Katsuhiko Mikoshiba[b,c,*]

[a] Department of Physiology, Juntendo University Faculty of Medicine, 2-1-1 Hongo, Bunkyo-ku, Tokyo 113-8421, Japan

[b] Calcium Oscillation Project, ICORP-SORST, Japan Science and Technology Agency (JST), 4-1-8 Honcho Kawaguchi, Saitama 332-0012, Japan

[c] Laboratory for Developmental Neurobiology, Brain Science Institute, RIKEN, 2-1 Hirosawa, Wako, Saitama 351-0198, Japan

[d] Department of Clinical Research and General Medicine, Yotsukaido Tokusyukai Medical Center, 1830-1 Yoshioka, Yotsukaido, Chiba 284-0032, Japan

Keywords: Ca^{2+} signaling; Ca^{2+} oscillation; muscarinic acetylcholine receptor

Abbreviations: BSS, balanced salt solution; mAChR, muscarinic acetylcholine receptors

* Corresponding author at: 2-1 Hirosawa, Wako, Saitama 351-0198, Japan, Phone: +81-48-467-9745, Fax: +81-48-467-9744

E-mail address: mikosiba@brain.riken.jp (K. Mikoshiba)

ABSTRACT

We examined ACh-induced $[Ca^{2+}]_i$ dynamics in pancreatic acinar cells prepared from mAChR subtype-specific knockout (KO) mice. ACh did not induce any $[Ca^{2+}]_i$ increase in the cells isolated from M1/M3 double KO mice. In the cells from M3KO mice, ACh (0.3 - 3 μM) caused a monotonic $[Ca^{2+}]_i$ increase. However, we found characteristic oscillatory $[Ca^{2+}]_i$ increases in cells from M1KO mice in lower concentrations of ACh (0.03 - 0.3 μM).

We investigated the receptor specific pattern of $[Ca^{2+}]_i$ increase in COS-7 cells transfected with M1 or M3 receptors. ACh induced the oscillatory $[Ca^{2+}]_i$ increase in M3 expressing cells, but not in cells expressing M1, which exhibited monotonic $[Ca^{2+}]_i$ increases. IP_3 production detected in fluorescent indicator co-transfected cells was higher in M1 than in M3 expressing cells. From the examination of four types of M1/M3 chimera receptors we found that the carboxyl-terminal region of M3 was responsible for the generation of Ca^{2+} oscillations.

The present results suggest that the oscillatory Ca^{2+} increase in response to M3 stimulation is dependent upon a moderate IP_3 increase, which is suitable for causing Ca^{2+}-dependent IP_3-induced Ca^{2+} release. The C-terminal domain of M3 may contribute as a regulator of the efficiency of Gq and PLC cooperation. (199 words)

1. Introduction

The pancreatic acinar cell has been widely employed by researchers as an experimental model for studying the contribution of muscarinic receptors to its exocrine functions [1-4]. Early studies demonstrated that exocrine pancreas secretion is mediated by the M3 receptor subtype [5-9]. This conclusion was based on radioligand binding and functional studies using antagonists for specific muscarinic receptors. However, the subtype specificity of these antagonists is limited. Therefore, the possibility exists that other mAChR subtypes may also contribute to mAChR mediated secretion.

Most sophisticated classifications of mAChRs contributing to secretion have been conducted by using pancreatic acinar cells isolated from M1 and/or M3 receptor knockout mice by Gautam et al. [10]. Based on that strategy, they demonstrated that cholinergic stimulation of pancreatic amylase secretion is mediated by a mixture of M1 and M3 mAChRs and that other mAChR subtypes do not make a significant contribution to this activity. Their report also showed that the efficiency of enzyme secretion in response to ACh was higher in cells isolated from M1KO than that from M3KO mice.

Since the exocrine system has been proven to be activated by intracellular Ca^{2+} ($[Ca^{2+}]_i$) increases induced by Gq-coupled mAChRs [10-13], it is important to address the distinct difference in $[Ca^{2+}]_i$ dynamics between M1 and M3 expressing cells. In particular, we need to concentrate on the oscillatory change in $[Ca^{2+}]_i$, which is actively utilized in releasing transmitters and hormones. [14-17].

In the present study, we examined $[Ca^{2+}]_i$ dynamics in acinar cells obtained from M1 and/or M3 mAChR knockout mice and also in COS-7 cells transfected with plasmids for M1 or M3 mAChRs with special reference to Ca^{2+} oscillations. To gain further

insight into the molecular mechanisms underlying Ca^{2+} oscillations, we tried to determine the critical receptor region by preparing M1 and M3 chimeric receptors.

2. Methods

All experiments were carried out in accordance with the guidelines approved by animal experimentation committees in our institutions.

2.1. Mice

Wild type mice (C57BL/6 strain) were purchased from CLEA (Tokyo, Japan). The generation and characterization of M1 and/or M3 knockout (KO) mice were performed according to procedures previously reported by Matsui et al. [18] and Ohno-Shosaku et al. [19]

2.2. Composition of the medium for in vitro experiments

We used balanced salt solution (BSS) containing 115 mM NaCl, 5.4 mM KCl, 2 mM $CaCl_2$, 1 mM $MgCl_2$, 20 mM HEPES, and 10 mM glucose, pH 7.4 for following *in vitro* experiments unless otherwise stated.

2.3. Preparation of pancreatic acinar cells.

Following anesthesia by pentobarbital (40 - 50 mg/kg, i.p.) and heart puncture, the pancreases of adult mice (3 - 4 months old) were immediately removed. The pancreases were placed in a cold Ca^{2+}-free BSS supplemented with 0.125% bovine serum albumin (Ca^{2+}-free BSS-BSA) and rapidly minced. The mince was then digested in 10 ml Ca^{2+}-free BSS containing 2 mg/ml collagenase type-1 (Worthington, Malvern, PA, USA) for 20 min at 37°C with 20 strokes of gentle pipetting every 10 min. After digestion, the preparation was passed through a 100 μm nylon mesh and washed three times by rinsing with Ca^{2+}-free BSS followed by centrifugation at 800 rpm for 1 min.

The pancreatic cell homogenates were digested with 0.5 mg/ml trypsin (Sigma) for 1 - 2 min at 37ºC in BSS-BSA. After 3 washes with Ca^{2+}-free BSS, the pancreatic cell homogenates were treated again with 2 mg/ml collagenase in Ca^{2+}-free BSS for 3 min at 37°C, washed twice with Ca^{2+}-free BSS, and further washed twice with normal BSS.

2.4. Preparation of plasmids for M1, M3 and M1/M3 chimeric receptors.

M1 and M3 receptor plasmid: The cDNA-encoding human M1 and M3 receptors (kind gift from Dr. Tatsuya Haga, Gakushuin University) was subcloned into the mammalian expression vector pcDNA3.1/zeo(+) (Invitrogen). The PCR (polymerase chain reaction) products of M1 and M3 were digested with *BamH*I/*EcoR*I and *Nhe*I/*EcoR*I, respectively.

M1/M3 chimeric receptor plasmid: To construct chimeric receptor genes containing fusions of coding sequences, PCR was used to amplify selectively DNA fragments encoding portions of M1 or M3 from plasmids containing the human M1 and M3 genes. In each case the 5' portion of the chimera was amplified with a forward primer encoding a unique restriction site (BamHI for M1 or NheI for M3) and the amino-terminal portion of the chimeric mAChR. The reverse primer for this fragment includes 20 bases at the site of the fusion. The 3' portion of each hybrid receptor gene was amplified with a forward primer including the fusion site, while the reverse primer for this fragment encoded a second unique restriction site (EcoRI) and the carboxyl terminus of the chimeric receptor. To obtain the full length of the chimeric gene, PCR was carried out to fuse the resultant fragments including 5' and 3’ portions. The products were digested with *BamH*I/*EcoR*I or *Nhe*I/*EcoR*I and ligated with pcDNA3.1/zeo(+). The primers used are summarized in Supplementary Table.1. All constructs were confirmed by DNA sequencing.

2.5. Transfection of M1, M3 or each M1/M3 chimeric receptor into COS-7 cells.

COS-7 cells were cultured in DMEM (Nacalai, Japan) supplemented with 10 % fetal bovine serum, 50 units/ml penicillin and 50 mg/ml streptomycin and plated on 35 mm poly-L-lysine-coated glass-bottom dishes 24 h before transfection. Prepared plasmid DNA (1 μg) for M1, M3 or each M1/M3 chimeric receptor was transfected using TransIT-LT1 (Mirus) following the protocol recommended by the manufacturer.

2.6. Ca^{2+} imaging of pancreatic acinar cells and COS-7 cells.

The isolated pancreatic acinar cell suspension was loaded with fura-2 by incubation for 45 min at room temperature with 3 μM fura-2-AM (Dojindo, Kumamoto, Japan) suspended in BSS-BSA. Then the cells were rinsed twice, and re-suspended in 4 ml of BSS. A small aliquot (20 - 50 μl) of fura-2 loaded pancreatic cells was dispersed on a Cell-Tak (BD Bioscience)-coated glass forming the bottom of the recording chamber, mounted on the stage of an inverted fluorescence microscope (Nikon TE300) (Nikon, Tokyo, Japan), and perfused with BSS at a rate of 2 ml/min at room temperature. Fluorescence images (510-550 nm emission) of fura-2 loaded cells induced by 340 and 380 nm excitation lights were detected every 5 sec by an oil immersion objective lens (S Fluor 40× N.A. 1.3) (Nikon, Tokyo, Japan) and a cooled CCD camera (ORCA-ER) (Hamamatsu Photonics, Shizuoka, Japan). The fluorescence images were processed by using AQUA-COSMOS/ratio software (Hamamatsu Photonics, Shizuoka, Japan) to obtain the F340/F380 ratio images.

COS-7 cells expressed plasmid DNA for specific receptors were loaded with 5 μM fura-2-AM in BSS for 30 min at room temperature 24 h after transfection, washed twice

with BSS and subjected to the same fluorescence image analysis as that for pancreatic acinar cell under the same experimental conditions using a 20× objective lens (S Fluor 20× N.A. 0.75) (Nikon, Tokyo, Japan).

2.7. Analysis of Ca^{2+} dynamics.

The relative change of the fura-2 F340/F380 ratio (ΔR) was calculated. We defined a response that had three or more peaks (with or without a plateau) during the 2-min agonist application as a Ca^{2+} oscillation. All values are presented as mean ± S.E.M. and error bars show S.E.M. Statistical differences were assessed by a Mann-Whitney U-test (Excel, Microsoft; StatPlus, AnalystSoft) or a Kruskal-Wallis test followed by Dunn's *post-hoc* test (GraphPad Prism4, GraphPad Software).

2.8. Western blotting of HA-tagged M1 or M3 receptors.

We plated COS-7 cells on 24-well plates and transfected HA-tagged M1, M3 and control pCMV-HA vectors. After 48 h the cells were harvested in sodium dodecyl sulphate sample buffer and boiled for 3 min. The resulting samples were applied to 7.5% PAGE gels in preparation for western blotting. The separated proteins were transferred to polyvinylidene difluoride (PVDF) membranes in a Transblot-Cell (Bio Rad Laboratories, Hercules, CA, USA). The membranes were then blocked with skimmed milk, washed and incubated with HA (1:1000, Roche) antibody for 1 h. After washing three times, the cells were incubated with anti-rat HRP-IgG (1:1000) for 1 h. Detection was performed with an ECL kit (GE Healthcare). Luminescence was recorded with an LAS-4000 mini biomolecular imager (LAS-4000, Fujifilm, Tokyo, Japan). For immunocytochemistry, we plated COS-7 cells on sterilized cover slips and transfected

HA-tagged M1 or M3 vector constructed with pCMV-HA vectors (Clontech). After 48 h, cells were fixed in 4% paraformaldehyde. After washing the cells with phosphate-buffered saline (PBS) twice, we treated cells with 50 mM NH_4Cl and 0.1% gelatin-PBS at room temperature. Cells were incubated with anti-HA antibody (1:1000, 3F10, Roche) for 1 h. After washing three times, we incubated cells with Alexa Fluor 488 IgG (1:1000) for 1 h and then cells were treated with 1 μg/ml of Hoechst 33342 for 15 min. We observed fluorescence signals using the FV1000 confocal laser scanning microscope (Olympus, Japan).

2.9. Imaging of GFP-PHD in COS-7 cells co-expressing the M1 or M3 receptor.

The fluorescent indicator, green fluorescent protein-tagged pleckstrin homology domain (GFP-PHD) of PLC-δ1, which permits real-time monitoring of IP_3 production, was constructed by subcloning the amino-terminal PH domain (1 - 140 or 11 - 140 amino acids) of rat phospholipase C delta into the EGFP-C1 vector (Clontech) [20]. All constructs were confirmed by DNA sequencing.

The fluorescent indicator EGFP-PHD was co-transfected with M1 or M3 in COS-7 cells. After 24 h, cells were mounted on the stage of an inverted fluorescence microscope (Nikon TE300) and imaged using the same conditions as those used for Ca^{2+} imaging of COS-7 cells. EGFP was excited every 2 sec by illumination with 480 nm light, and the resulting fluorescence (515-560 nm) was collected with an objective lens (40×, oil) and a cooled CCD camera and processed with AQUA-COSMOS/ratio software (Hamamatsu Photonics, Shizuoka, Japan).

The Hill plot, Hill co-efficient and ED_{50} for M1 and M3 receptor mediated increase in fluorescence of EGFP were calculated using SigmaPlot 10.

3. Results

3.1. Ca^{2+} imaging of single pancreatic acinar cells.

To investigate the subtype contribution to ACh-evoked Ca^{2+} signaling in pancreatic acinar cells, we performed fura-2 Ca^{2+} imaging of single pancreatic acinar cell prepared from wild-type (WT), M1KO, M3KO, M1/M3 double KO mice. As shown in Fig.1A, the cells isolated from WT and M1KO showed dose-dependent increases in $[Ca^{2+}]_i$ to ACh (0.03 - 0.3 μM). Almost all of the cells showed clear increases in $[Ca^{2+}]_i$ to ACh (0.3 μM) (Supplementary Fig. S1). We observed characteristic oscillatory $[Ca^{2+}]_i$ increases among responding cells in relatively lower concentrations of ACh. However, the ratio of cells showing oscillatory responses declined at the highest concentration of 0.3 μM in WT (Fig. 1C). The pattern of response to ACh in cells obtained from M1KO mice was almost the same as those observed in cells from WT.

On the other hand, the cells isolated from M3KO mice showed poor responses to ACh (Fig. 1A and B). Dose-dependent responses to ACh of these cells were observed in a much higher dose range (0.3 - 3 μM). Estimating from the ACh (3 μM) responding cells, the population of acinar cells expressing M1 receptor was less than 50% of M3 expressing cells (Supplementary Fig. S1). Although we could observe oscillatory responses in a few cells at 1.0 μM, there was no oscillatory response in cells treated with 0.3 and 3.0 μM ACh (Fig. 1C). The maximum size of the $[Ca^{2+}]_i$ increase in response to the highest tested concentration (3 μM) in cells from M3KO mice was the same as that of the $[Ca^{2+}]_i$ response induced by 0.3 μM in those from M1KO mice (Fig. 1B).

The cells isolated from M1/M3 double KO mice showed no significant responses to ACh even at the highest dose (3 μM) (Fig. 1A). These results suggest that the receptor

subtypes participating in the $[Ca^{2+}]_i$ responses to ACh were M1 and M3, and that the other mAChRs did not make a significant contribution to this activity in pancreatic acinar cells.

These results suggest that M3 is the major subtype responsible for ACh-evoked Ca^{2+} responses in acinar cells, but the contribution of M1 seems to be minor, accounting for the small residual ACh-evoked responses observed in M1 cells. Our findings indicate that M3 is necessary for the generation of ACh-evoked Ca^{2+} oscillations in acinar cells, and that M1 mediates non-oscillatory Ca^{2+} increases. However, since the response of M1 in pancreatic acinar cells to ACh was apparently lower than that of M3 in pancreatic acinar cells, it is necessary to address the subtype specificity of Ca^{2+} oscillation induction in cells expressing comparable amount of M1 and M3.

3.2. Ca^{2+} imaging of COS-7 cells heterologously expressing M1 or M3.

We prepared COS-7 cells heterologously expressing either M1 or M3. The responses of these cells to ACh were compared to examine whether the marked difference between M1 and M3 in the generation of $[Ca^{2+}]_i$ oscillations is attributable to the intrinsic properties of these receptor subtypes or cellular distribution. We confirmed that COS-7 cells themselves do not express functional ACh receptors on the cells transfected with the control vector (pcDNA3.1/zeo(+)) because they did not show any Ca^{2+} responses to ACh, although the cells responded to 3 μM ATP and thus were viable (Fig. 2A).

We found that cells transfected with M1 or M3 showed dose dependent increases in $[Ca^{2+}]_i$ over almost the same range of ACh concentrations (1 - 10 nM) (Fig. 2A and B). ACh induced larger increases in $[Ca^{2+}]_i$ in M3 than M1 expressing cells at lower concentrations (1 and 3 nM). The incidence of the $[Ca^{2+}]_i$ oscillations observed in M3

cells was higher in 1 nM than in 10 nM ACh. We observed $[Ca^{2+}]_i$ oscillations in M1 expressing cells in a few cells exposed to higher concentration of ACh (3 - 10 nM) (Fig. 2C).

We confirmed in a separate experiment using HA-tagged M1 and M3 plasmids that the expression level was almost comparable to or higher in M1 than M3 when transfected with the same concentration as that used in Ca^{2+} imaging (Fig. 3A). We also confirmed the similar expression levels of these receptors at the cell periphery by using anti-HA antibody (Fig. 3B and supplementary Fig. S2).

The sensitivity of COS-7 cells with M1 or M3 receptors was high compared to wild acinar cells, presumably reflecting relatively higher expression of receptor proteins in the over-expression system.

These results suggest that M3 but not M1 contribute to the generation of Ca^{2+} oscillations, and that this marked difference cannot be attributed to the difference in the expression level alone. Although the responses of M1 and M3 expressing cells to ACh seemed to be reduced by extracellular Ca^{2+} deprivation, the intrinsic profiles in $[Ca^{2+}]_i$ dynamics were not influenced in the condition suggesting that the source of $[Ca^{2+}]_i$ was the intracellular store site (see supplementary Fig. S3).

3.3. Changes in GFP-PHD fluorescence by ACh-induced IP_3 production.

Next, we measured IP_3 production with the fluorescent indicator EGFP-PHD, which can be used to assess IP_3 production by translocation of EGFP-PHD from the cytoplasmic membrane to the cytosolic space [20]. We observed significant decreases in the fluorescence intensity at the cytoplasmic membrane and reciprocal increases in cytosolic fluorescence during stimulation with 0.1 μM ACh in COS-7 cells

co-expressing EGFP-PHD and the muscarinic receptors (Fig. 4A). The time-series of the fluorescent images and measured intensities clearly demonstrate that the translocation was reversible, as indicated by the arrows in Fig. 4A. We confirmed that an indicator lacking the PH domain did not exhibit a response to 0.1 μM ACh in M1- or M3-expressing cells. When no muscarinic receptor was transfected, no translocation of EGFP-PHD by ACh was observed because there was no endogenous ACh receptor (Supplementary Fig. S4). These results indicate that the EGFP-PHD translocation rigorously monitors the ACh-evoked IP_3 signaling through heterologously expressed M1 or M3 receptors. The COS-7 cells co-expressing EGFP-PHD and muscarinic receptors were stimulated with 3, 10 and 30 nM ACh (Fig. 4B), and $\Delta F/F_0$ was calculated from the fluorescence intensities at 480 nm of cytosolic EGFP-PHD (3, 10, 30 and 100 nM ACh) in M1-expressing cells (n = 4 - 27 cells at each concentration) or M3-expressing cells (n = 4 - 10 cells at each concentration) (Fig. 4C). The summary plot indicates a marked difference between the M1 (blue) and M3-dependent (red) responses. The EC_{50} of M3-mediated translocation of EGFP-PHD was 21.2 nM with a Hill coefficient of 1.0, whereas that of M1 was 7.91 nM with Hill coefficient of 2.3.

It is worth noticing that there was no oscillation in the EGFP-PHD fluorescence dynamics in both M1 and M3-expressing cells.

3.4. Ca^{2+} imaging of COS-7 cells heterologously expressing M1/M3 chimeric receptors.

To gain further insights into the molecular mechanisms underlying Ca^{2+} oscillations, we tried to determine the critical receptor region(s) by making M1/M3 chimeric receptors. An M1/M3 chimera was constructed by fusing the N-terminal half of human M1 (1 - 214 amino acids) with the C-terminal half of M3 (258 - 590 amino acids); an M3/M1

chimera by fusing the N-terminal moiety of M3 (1 - 257 amino acids) with the C-terminal half of M1 (215 - 460 amino acids); an M1/M3C chimera by fusing the large N-terminal part of M1 (1 - 368 amino acids) with the small C-terminal region of M3 (495 - 590 amino acids); and an M3/M1C chimera by fusing the large N-terminal part of M3 (1 - 494 amino acids) with the small C-terminal portion of M1 (369 - 460 amino acids).

We examined ACh-induced $[Ca^{2+}]_i$ increase in COS-7 cells transfected with each chimera (Fig. 5). As shown in Fig. 5A, cells expressing each of the four chimera receptors had almost equal size responses, and showed a similar dose-response relationship to 1, 3 and 10 nM ACh (Fig. 5B). However, we observed a high population of cells with obvious oscillatory responses to ACh among the cells expressed M1/M3 or M1/M3C chimera receptor. On the other hand, M3/M1 or M3M1C chimera transfected cells showed no or only a few Ca^{2+} oscillations. The dose-response relationships for the ratio of oscillatory cells to ACh (1, 3 and 10 nM) were bell shaped in M1/M3, M1/M3C and M3/M1C expressing cells.

4. Discussion

4.1. M1 and M3 contribution to physiological function in exocrine glands.

In the present study we found a distinct contribution of M1 and M3 receptors to the increase in $[Ca^{2+}]_i$ in freshly isolated pancreatic acinar cells obtained from M1 and/or M3 knockout mice. Since the M1 and M3 double knockout mice did not show any increase in $[Ca^{2+}]_i$ following stimulation with high concentrations of ACh, we confirmed that M1 and M3 subtypes were the major muscarinic receptors linked to Ca^{2+} increases in pancreatic acinar cells. The expression and apparent affinity to ACh of the M3 receptor were higher than those of the M1 receptor. The oscillatory response to ACh at lower concentrations was observed almost exclusively in the M3 expressing cells, and the percentage of the cells with an oscillatory response tended to decrease or reached a plateau in higher concentrations of ACh, which suggests that there is an optimal level of $[Ca^{2+}]_i$ for inducing an oscillatory Ca^{2+} release which is a characteristic property of Ca^{2+}-dependent IP_3-induced Ca^{2+} release (IICR).

Our findings confirmed the results reported by Gautam et al. [10], who demonstrated the different contribution of M1 and M3 expressed in pancreatic acinar cells to the release of amylase by using isolated acinar cells obtained from the knockout mice. They showed a bell-shaped dose response curve to carbachol in WT and M1KO cells. Their data demonstrated that the sensitivity to carbachol of M1KO cells was significantly higher than that of M3KO cells. The bell shaped dose-response relationship seems to be dependent upon oscillatory $[Ca^{2+}]_i$ induced through the activation of M3 receptors in acinar cells. Monotonic increases in $[Ca^{2+}]_i$ observed in both M1 and M3 expressing cells by higher concentrations of ACh would be utilized as the trigger for the releasing system, but the efficiency might be lower than that of the oscillatory increase.

Oscillatory changes in $[Ca^{2+}]_i$ have also been reported in the other releasing systems [14-17].

4.2. $[Ca^{2+}]_i$ responses to ACh in COS-7 cells with artificially expressed M1 and M3 receptors.

The $[Ca^{2+}]_i$ response to ACh in acinar cells isolated from M3KO mice was unexpectedly low. Since we used collagenase treatment in the process of isolating the cells, some portion of M1 might have deteriorated. The apparent poor responses and expression of M1 might be the results of the procedure. It may be too early to determine the properties of M1 and M3 receptors from the results on cells from knockout mice. We prepared M1 or M3 expressing COS-7 cells, which do not express intrinsic ACh receptors, using the same amount of expression vectors, and examined the $[Ca^{2+}]_i$ responses in M1 and M3. The sensitivity of these cells to ACh was very high, and almost similar dose-response relationships were obtained. The results demonstrated that the $[Ca^{2+}]_i$ response to ACh in M1 or M3 expressing cells were substantially the same as those observed in cells isolated from M1KO or M3KO mice, which indicates that the pattern of $[Ca^{2+}]_i$ increase is dependent upon the receptor subtype.

4.3. Estimation of IP_3 production in EGFP-PHD expressed M1 or M3 mACh expressing COS-7 cells.

Oscillations in $[Ca^{2+}]_i$ induced by G-protein coupled receptors have been demonstrated to be dependent upon two distinct mechanisms. One of those is the self-propagating action of Ca^{2+} on IP_3 receptors (IICR) [21], and the other is the dynamic uncoupling and recoupling process of the PLC/IP_3 signaling pathway [22].

IP_3 production was estimated using imaging analysis of the translocation of green fluorescent protein (GFP)-tagged pleckstrin homology domain EGFP-PHD transfected COS-7 cells with M1 or M3 [20]. As has been reported by Nash et al. [23], there was no oscillatory change in IP_3 production during the activation with ACh in M1 as well as M3 mAChR cells, which means the oscillation in $[Ca^{2+}]_i$ might not be dependent on the uncoupling and recoupling process in PLC/IP_3 signaling through phosphorylation control [24], but dependent on classical Ca^{2+}-dependent IICR process, which will be induced in lower $[Ca^{2+}]_i$. The EC_{50} of the M3-mediated translocation of EGFP-PHD was 21.3 nM with a Hill coefficient of 1.0, whereas that of M1 was 7.1 nM with a Hill coefficient of 2.3. The results apparently demonstrated that M1 receptor was more efficient for producing IP_3 than M3 receptor. However, the dose-response curves fitted according to the responses obtained by tested doses suggested that the efficiency of IP_3 production by M3 receptor might be higher to lower ACh concentrations, which were effective to cause Ca^{2+} release from ER (Fig. 2B).

The result is an important clue confirming that the oscillatory $[Ca^{2+}]_i$ increase in M3 cells induced by lower ACh concentrations might be dependent on the release of a low but sufficient amount of IP_3 to activate the Ca^{2+} dependent IP_3 induced Ca^{2+} release. Although the Hill coefficient of GFP-PHD translocation (IP_3 production) in M1 cell was very high, the response to the lower ACh concentration might be too low to activate the IP_3 receptor to cause IICR. And the level of IP_3 induced by high concentration of ACh was too high to promote the Ca^{2+} oscillation. However, to confirm this speculation, we need a method with much higher sensitivity for IP_3 released during M1 and M3 receptor stimulation.

In rare cases, when the IP_3 level might match the critical level for activating Ca^{2+}

dependent IICR, Ca^{2+} oscillation could be observed by M1 receptor stimulation (Fig. 2C).

4.4. The molecular mechanisms underlying distinct Ca^{2+} dynamics evoked by M1 and M3 by M1/M3 or M3/M1 chimera receptors.

In order to investigate the molecular mechanisms underlying the difference in $[Ca^{2+}]_i$ dynamics between M1 and M3 regarding the generation of IP_3, we examined the efficiency of chimera receptors taking the observation of an oscillation in $[Ca^{2+}]_i$ as an index. Our data on M1/M3 and M3/M1 chimera receptors indicate that the C-terminal portion of M3 containing the 3rd intracellular loop (i3 loop), 6th and 7th trans-membrane domains, 4th extracellular domain and the C-terminal tail may be critical for the generation of Ca^{2+} oscillations. However, data on M1/M3C and M3/M1C chimera receptors showed that the domain containing the C-terminal tail alone seemed to be crucial for the generation of Ca^{2+} oscillations. This domain shows high variability in amino acid sequences among subtypes. The i3 loop, which is responsible for Gq-binding [25, 26], consists of a small segment conserved among subtypes and a subtype-specific large segment [27]. It is conceivable that the interaction among subtype-specific segments in the i3 loop and/or C-terminal tail could contribute to the mechanism underlying IP_3 production with some regulator proteins binding to these domains with different efficiency. RGS2, an activator of GTPase, which has been reported to bind directly to the i3 loop of M1 [28] and to downregulate the frequency of ACh-evoked Ca^{2+} oscillations in pancreatic acinar cells [29], may be one of the regulator candidates. However, our findings on chimera receptors suggest that the contribution of the C-terminal region in generating oscillations was much higher than

that of i3 loop. Further study is required to elucidate how the C-terminal tail participates in the regulation of the interaction between the G-protein and PLC to control IP_3 production.

Overall, we conclude that the oscillatory $[Ca^{2+}]_i$ increase induced by ACh in M3 expressing cells is mediated by a moderate level of Gq and PLC cooperation in a wide dose range, which is regulated by the C-terminal domain to produce an optimal level of IP_3 to cause Ca^{2+} oscillation.

Conflict of interest

The authors declare no conflict of interests.

Acknowledgment

We greatly appreciate Dr. Tatsuya Haga (Gakushuin Univ.) for his gift of human M1/M3 plasmids. We thank Dr. Mitsuharu Hattori (Nagoya City Univ.) for the EGFP-PHD plasmid. We thank Drs. Yoshihisa Kudo (Tokyo Univ. of Pharmacy and Life Science), Makino Watanabe (Juntendo Univ.) and Yoshiyuki Yamada (RIKEN) for useful discussions; Nagisa Matsumoto for technical assistance, and the RIKEN Research Resources Center (RRC) for providing common-use equipments. This work was supported by grants from the Ministry of Education, Science and Culture of Japan to K.M. (20220007) and ICORP-SORST of JST.

References

[1] T.E. Solomon, Regulation of pancreatic secretion, Clin Gastroenterol, 13 (1984) 657-678.

[2] C.C. Petersen, E.C. Toescu, O.H. Petersen, Different patterns of receptor-activated cytoplasmic Ca^{2+} oscillations in single pancreatic acinar cells: dependence on receptor type, agonist concentration and intracellular Ca^{2+} buffering, EMBO J, 10 (1991) 527-533.

[3] Y. Fukushi, I. Kato, S. Takasawa, T. Sasaki, B.H. Ong, M. Sato, A. Ohsaga, K. Sato, K. Shirato, H. Okamoto, Y. Maruyama, Identification of cyclic ADP-ribose-dependent mechanisms in pancreatic muscarinic Ca^{2+} signaling using CD38 knockout mice, J Biol Chem, 276 (2001) 649-655.

[4] O.H. Petersen, A.V. Tepikin, Polarized calcium signaling in exocrine gland cells, Annu Rev Physiol, 70 (2008) 273-299.

[5] D.S. Louie, C. Owyang, Muscarinic receptor subtypes on rat pancreatic acini: secretion and binding studies, Am J Physiol, 251 (1986) G275-279.

[6] M. Korc, M.S. Ackerman, W.R. Roeske, A cholinergic antagonist identifies a subclass of muscarinic receptors in isolated rat pancreatic acini, J Pharmacol Exp Ther, 240 (1987) 118-122.

[7] K. Iwatsuki, A. Horiuchi, H. Yonekura, N. Homma, K. Haruta, S. Chiba, Subtypes of muscarinic receptors in pancreatic exocrine secretion in anesthetized dog, Pancreas, 4 (1989) 339-345.

[8] M. Kato, S. Ohkuma, K. Kataoka, K. Kashima, K. Kuriyama, Characterization of muscarinic receptor subtypes on rat pancreatic acini: pharmacological identification by secretory responses and binding studies, Digestion, 52 (1992) 194-203.

[9] J.A. Love, K. Szebeni, T.G. Smith, Veratridine-stimulated amylase secretion from rabbit pancreatic lobules: role of cholinergic and noncholinergic receptors, Pancreas, 19 (1999) 231-238.

[10] D. Gautam, S.J. Han, T.S. Heard, Y. Cui, G. Miller, L. Bloodworth, J. Wess, Cholinergic stimulation of amylase secretion from pancreatic acinar cells studied with muscarinic acetylcholine receptor mutant mice, J Pharmacol Exp Ther, 313 (2005) 995-1002.

[11] M. Wakui, Y.V. Osipchuk, O.H. Petersen, Receptor-activated cytoplasmic Ca^{2+} spiking mediated by inositol trisphosphate is due to Ca^{2+}-induced Ca^{2+} release, Cell, 63 (1990) 1025-1032.

[12] T. Nakamura, M. Matsui, K. Uchida, A. Futatsugi, S. Kusakawa, N. Matsumoto, K. Nakamura, T. Manabe, M.M. Taketo, K. Mikoshiba, M(3) muscarinic acetylcholine receptor plays a critical role in parasympathetic control of salivation in mice, J Physiol, 558 (2004) 561-575.

[13] O.H. Petersen, Ca^{2+} signalling and Ca^{2+}-activated ion channels in exocrine acinar cells, Cell Calcium, 38 (2005) 171-200.

[14] S.J. Smith, G.J. Augustine, Calcium ions, active zones and synaptic transmitter release, Trends Neurosci, 11 (1988) 458-464.

[15] H. Kasai, G.J. Augustine, Cytosolic Ca^{2+} gradients triggering unidirectional fluid secretion from exocrine pancreas, Nature, 348 (1990) 735-738.

[16] G.J. Augustine, E. Neher, Calcium requirements for secretion in bovine chromaffin cells, J Physiol, 450 (1992) 247-271.

[17] H. Kasai, Y.X. Li, Y. Miyashita, Subcellular distribution of Ca^{2+} release channels underlying Ca^{2+} waves and oscillations in exocrine pancreas, Cell, 74 (1993) 669-677.

[18] M. Matsui, D. Motomura, H. Karasawa, T. Fujikawa, J. Jiang, Y. Komiya, S. Takahashi, M.M. Taketo, Multiple functional defects in peripheral autonomic organs in mice lacking muscarinic acetylcholine receptor gene for the M3 subtype, Proc Natl Acad Sci U S A, 97 (2000) 9579-9584.

[19] T. Ohno-Shosaku, M. Matsui, Y. Fukudome, J. Shosaku, H. Tsubokawa, M.M. Taketo, T. Manabe, M. Kano, Postsynaptic M1 and M3 receptors are responsible for the

muscarinic enhancement of retrograde endocannabinoid signalling in the hippocampus, Eur J Neurosci, 18 (2003) 109-116.

[20] K. Hirose, S. Kadowaki, M. Tanabe, H. Takeshima, M. Iino, Spatiotemporal dynamics of inositol 1,4,5-trisphosphate that underlies complex Ca^{2+} mobilization patterns, Science, 284 (1999) 1527-1530.

[21] S. Miyazaki, Repetitive calcium transients in hamster oocytes, Cell Calcium, 12 (1991) 205-216.

[22] P. De Koninck, H. Schulman, Sensitivity of CaM kinase II to the frequency of Ca^{2+} oscillations, Science, 279 (1998) 227-230.

[23] M.S. Nash, K.W. Young, R.A. Challiss, S.R. Nahorski, Intracellular signalling. Receptor-specific messenger oscillations, Nature, 413 (2001) 381-382.

[24] S. Kawabata, R. Tsutsumi, A. Kohara, T. Yamaguchi, S. Nakanishi, M. Okada, Control of calcium oscillations by phosphorylation of metabotropic glutamate receptors, Nature, 383 (1996) 89-92.

[25] J. Wess, M.R. Brann, T.I. Bonner, Identification of a small intracellular region of the muscarinic m3 receptor as a determinant of selective coupling to PI turnover, FEBS Lett, 258 (1989) 133-136.

[26] J. Lechleiter, R. Hellmiss, K. Duerson, D. Ennulat, N. David, D. Clapham, E. Peralta, Distinct sequence elements control the specificity of G protein activation by muscarinic acetylcholine receptor subtypes, EMBO J, 9 (1990) 4381-4390.

[27] E.C. Hulme, N.J. Birdsall, N.J. Buckley, Muscarinic receptor subtypes, Annu Rev Pharmacol Toxicol, 30 (1990) 633-673.

[28] L.S. Bernstein, S. Ramineni, C. Hague, W. Cladman, P. Chidiac, A.I. Levey, J.R. Hepler, RGS2 binds directly and selectively to the M1 muscarinic acetylcholine receptor third intracellular loop to modulate Gq/11alpha signaling, J Biol Chem, 279 (2004) 21248-21256.

[29] X. Wang, G. Huang, X. Luo, J.M. Penninger, S. Muallem, Role of regulator of G

protein signaling 2 (RGS2) in Ca^{2+} oscillations and adaptation of Ca^{2+} signaling to reduce excitability of RGS2-/- cells, J Biol Chem, 279 (2004) 41642-41649.

FIGURE LEGENDS

Fig. 1. *Distinct Ca^{2+} dynamics in pancreatic acinar cells from mAChR KO mice.*
(A). Left panels show fura-2 fluorescence and pseudo-color images of F340/F380 under resting and ACh-stimulated conditions (0.3 μM in WT and M1KO; 3 μM in M3KO and M1/M3 double KO). At right are typical traces of $[Ca^{2+}]_i$ in response to ACh (0.03, 0.1 and 0.3 μM in WT and M1KO; 0.3, 1 and 3 μM in M3KO and M1/M3 double KO). Horizontal bars indicate the duration of ACh application. Vertical axis indicates the change in fura-2 ratio (ΔR). (B) The dose-response relationship to ACh in cells isolated from WT, M1KO (total 119 - 227 cells from 5 - 17 experiments, total 205 cells from 9 experiments) and M3KO (total 500 - 689 cells from 12 - 16 experiments). (C) The mean percentage (%) of oscillating cells of the total responding cells from WT, M1KO and M3KO. Statistical difference was assessed by Mann-Whitney U test. * $p < 0.05$, ** $p < 0.01$, *** $p < 0.001$.

Fig. 2. *Distinct ACh-evoked Ca^{2+} responses in COS-7 cells heterologously expressing either M1 or M3 receptors.*
(A) Typical traces of the $[Ca^{2+}]_{i,}$ response to ACh (1, 3 and 10 nM) in COS-7 cells expressing M1 (left) or M3 (middle). Right traces show responses of mock-transfected cells (pcDNA3.1/zeo(+)) to ACh (300 and 1000 nM) and 3 μM ATP. Note that M3-expressing COS7-cells (middle) generated ACh-induced Ca^{2+} oscillations, but M1-expressing COS-7 cells (left) show Ca^{2+} increases without obvious oscillations. (B) The dose-response relationship to ACh in M1- (total 21 - 89 responding cells from 7 experiments: filled column) and M3-transfected cells (total 200 - 311 responding cells from 10 to 16 experiments: open column). (C) Graph represents the mean ± S.E.M. of the percentage (%) of oscillating cells responded to ACh (1, 3 and 10 nM). Statistical difference was assessed by Mann-Whitney U test. * $p < 0.05$, ** $p < 0.01$, *** $p < 0.001$.

Fig.3 *The expression levels of M1 and M3 receptors in COS-7 cells.*
(A) The expression levels of HA-M1 or HA-M3 were detected by Western blotting with an anti-HA monoclonal antibody. Low (2/3×) and high (1×) expression levels of

HA-M1 were obtained by transfection with 2/3 μg and 1 μg of plasmid respectively. Low (1×) and high (3×) expression levels of HA-M3 obtained by transfection with 1.0 μg and 3.0 μg of plasmid, respectively. The mock transfection with the pCMV-HA vector is shown in the right lane. (B) Panels show the micrographs of COS-7 cells transfected with HA-M1 (1×) and M3 (3×). Green, anti-HA immunostain. Blue, Hoechst 33342 stain.

Fig 4. *Imaging of EGFP-PHD translocation by M1- or M3-mediated IP_3 production.*
(A) In the left panel, changes in the fluorescence of EGFP-PHD upon excitation at 480 nm at the cytoplasmic membrane (red line) or in the cytosolic space (black line) in response to 0.1 μM ACh as recorded in COS-7 cells co-expressing EGFP-PHD and M1. The right panel shows the fluorescence changes in COS-7 cells co-expressing EGFP-PHD and M3. The upper rows are the fluorescence images obtained at the times indicated by the arrows. (B) Typical trace of fluorescence intensity of cytosolic EGFP-PHD induced by various concentration of ACh (3, 10 and 30 nM) in M1 (left) and M3 cells (right). (C) Dose-response relationship of fractional changes ($\Delta F/F_0$) obtained from COS-7 cells co-expressing EGFP-PHD and M1 (blue) (n = 4 - 27 in each point) or M3 (red) (n = 4 - 10 in each point) in response to ACh (3, 10, 30 and 100 nM). The lines were fitted with the Hill equation.

Fig. 5. *Chimeric receptors generate distinct Ca^{2+} dynamics.*
(A) Representative traces of ACh-induced (1, 3 and 10 nM) Ca^{2+} responses in COS-7 cells transfected with M1/M3, M3/M1, M1/M3C or M3/M1C hybrid receptors. The structure of each chimera receptor is illustrated in the top row. (B) Dose-response relationship to ACh (1, 3 and 10 nM) in the cells expressing each hybrid receptor. Bar charts represent means ± S.E.M. of $[Ca^{2+}]_i$ increases with M1/M3 (total 135 - 270 responding cells from 11 to 12 experiments), M3/M1 (total 21 - 134 responding cells from 8 to 13 experiments) M1/M3C (total 91 - 274 responding cells from 10 experiments) and M3/M1C (total 48 - 115 responding cells from 7 experiments) hybrid receptors. (C) Graph represents the mean ± S.E.M. of the percentage (%) of oscillating cells responding to ACh (1, 3 and 10 nM). Statistical difference was assessed by Dunn's multiple comparisons following Kruskal-Wallis Test. * $p < 0.05$, ** $p < 0.01$, *** $p <$

0.001.

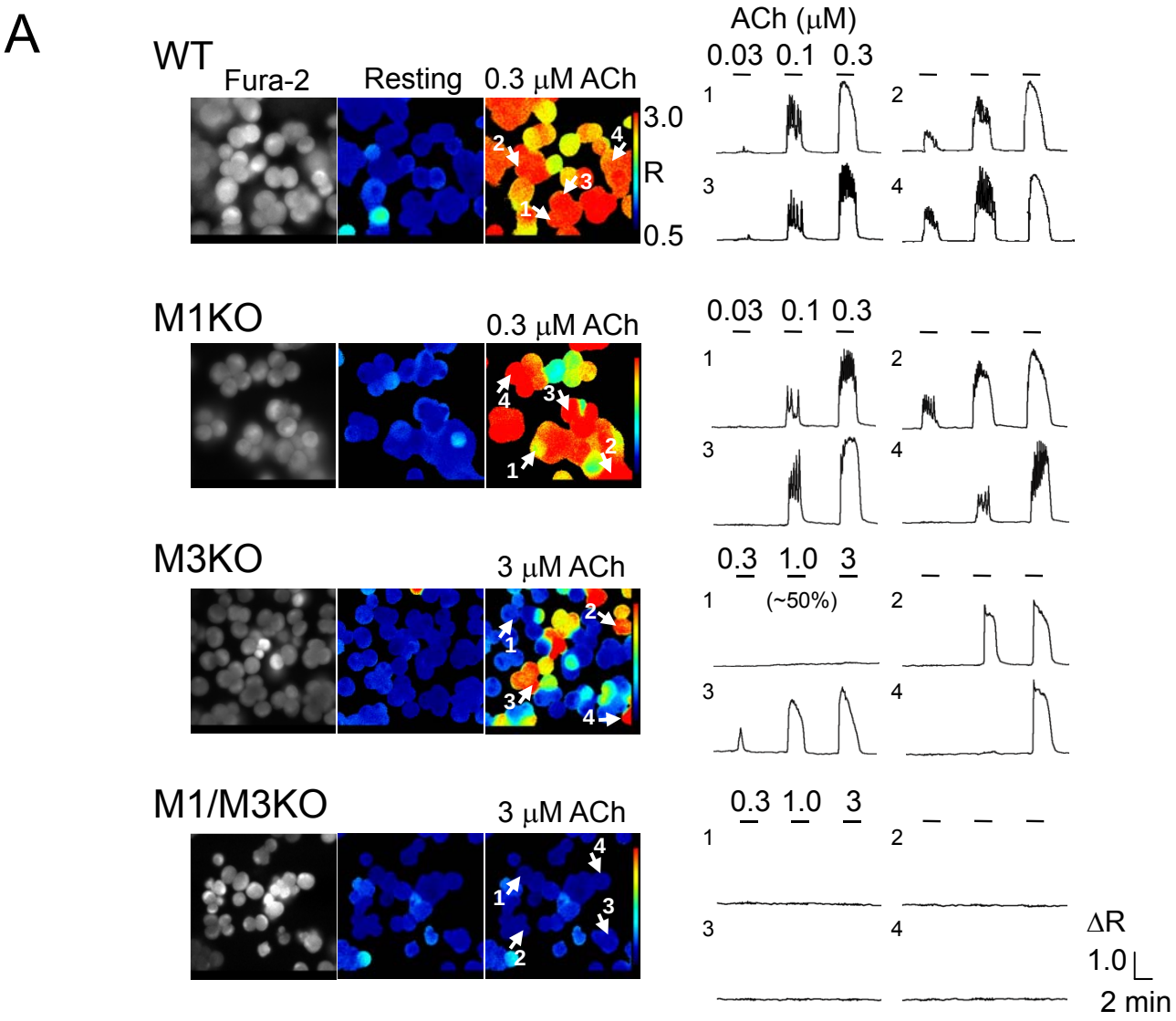
A
WT
Fura-2
Resting
0.3 μM ACh
3.0
R
0.5
ACh (μM)
0.03 0.1 0.3
M1KO
0.3 μM ACh
0.03 0.1 0.3
M3KO
3 μM ACh
0.3 1.0 3
(~50%)
M1/M3KO
3 μM ACh
0.3 1.0 3
ΔR
1.0
2 min

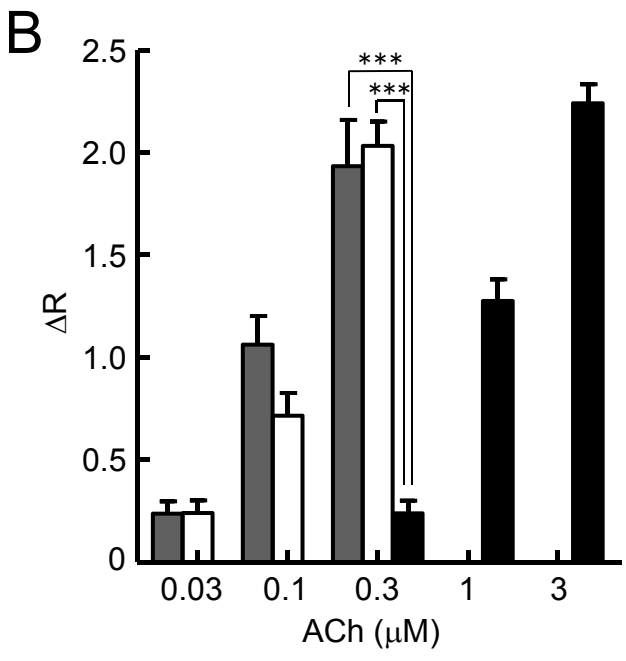
B
ΔR
2.5
2.0
1.5
1.0
0.5
0
***
***
0.03 0.1 0.3 1 3
ACh (μM)

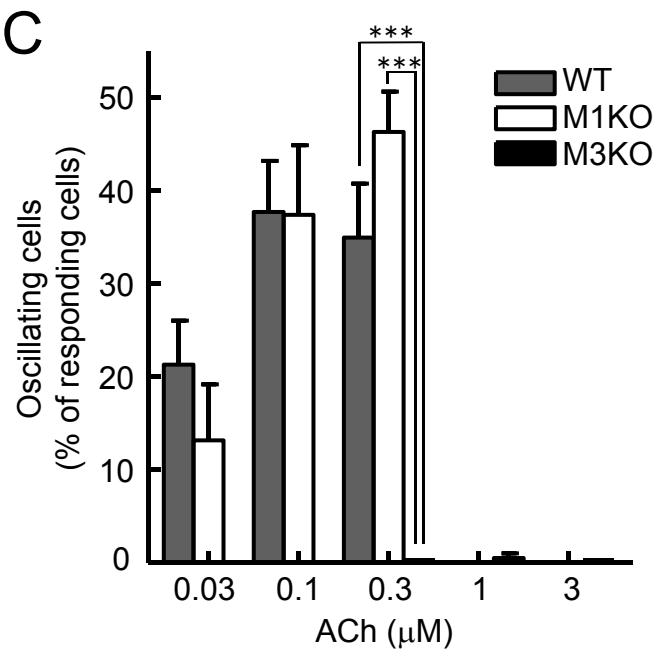
C
Oscillating cells
(% of responding cells)
50
40
30
20
10
0
***
***
WT
M1KO
M3KO
0.03 0.1 0.3 1 3
ACh (μM)

Fig. 1

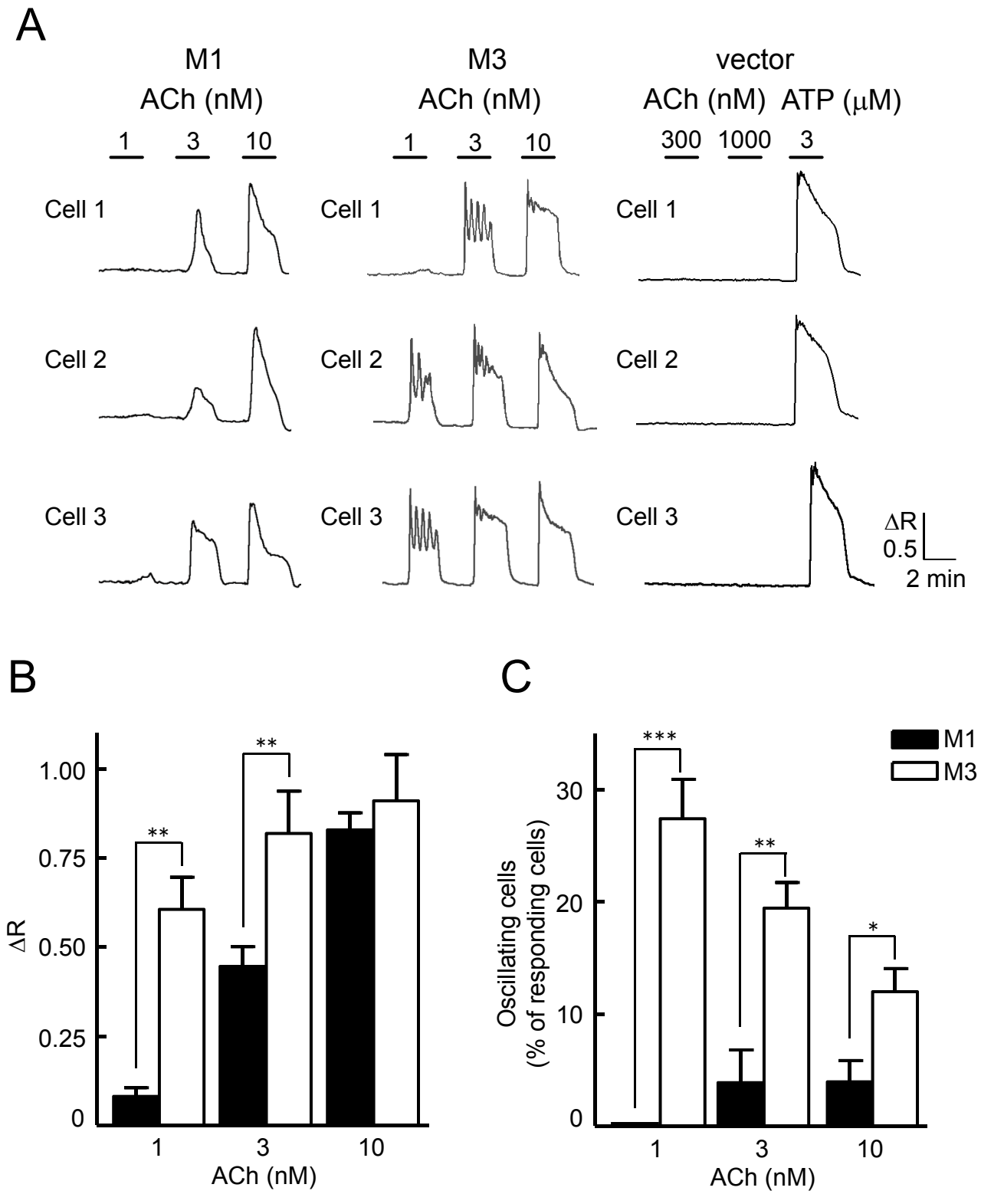
A
M1
ACh (nM)
1 3 10
M3
ACh (nM)
1 3 10
vector
ACh (nM) ATP (μM)
300 1000 3
Cell 1
Cell 2
Cell 3
ΔR
0.5
2 min
B
ΔR
1.00
0.75
0.50
0.25
0
**
**
1 3 10
ACh (nM)
C
Oscillating cells
(% of responding cells)
30
20
10
0
***
**
*
M1
M3
1 3 10
ACh (nM)

Fig. 2

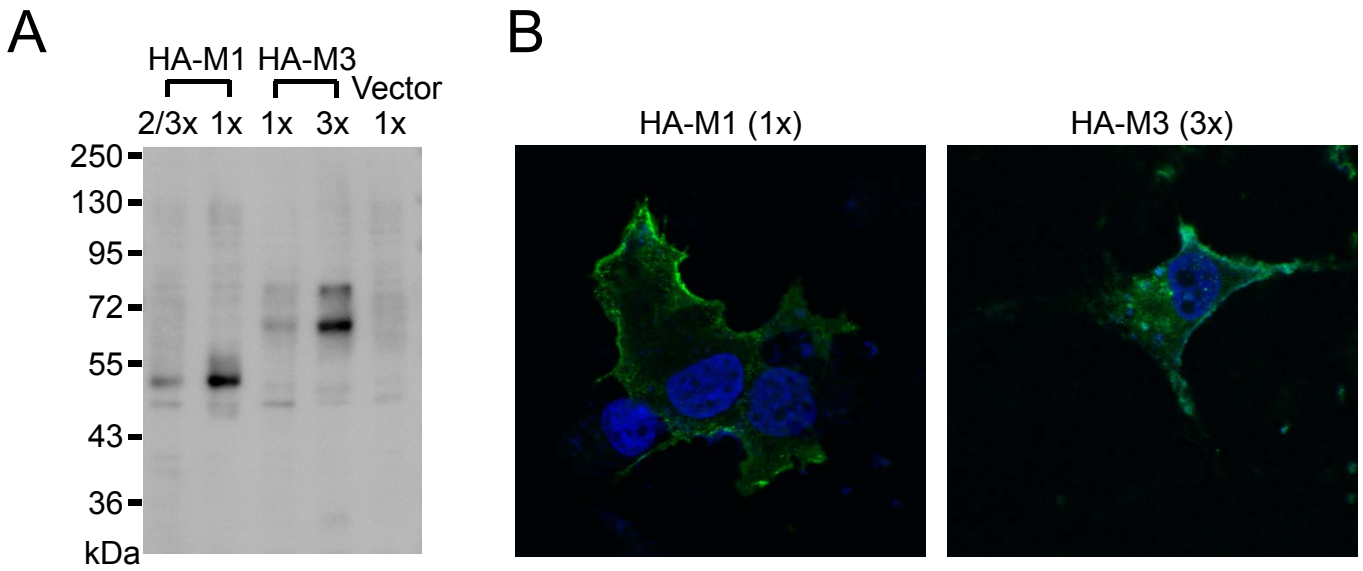
A
HA-M1
HA-M3
Vector
2/3x
1x
1x
3x
1x
250
130
95
72
55
43
36
kDa
B
HA-M1 (1x)
HA-M3 (3x)

Fig. 3

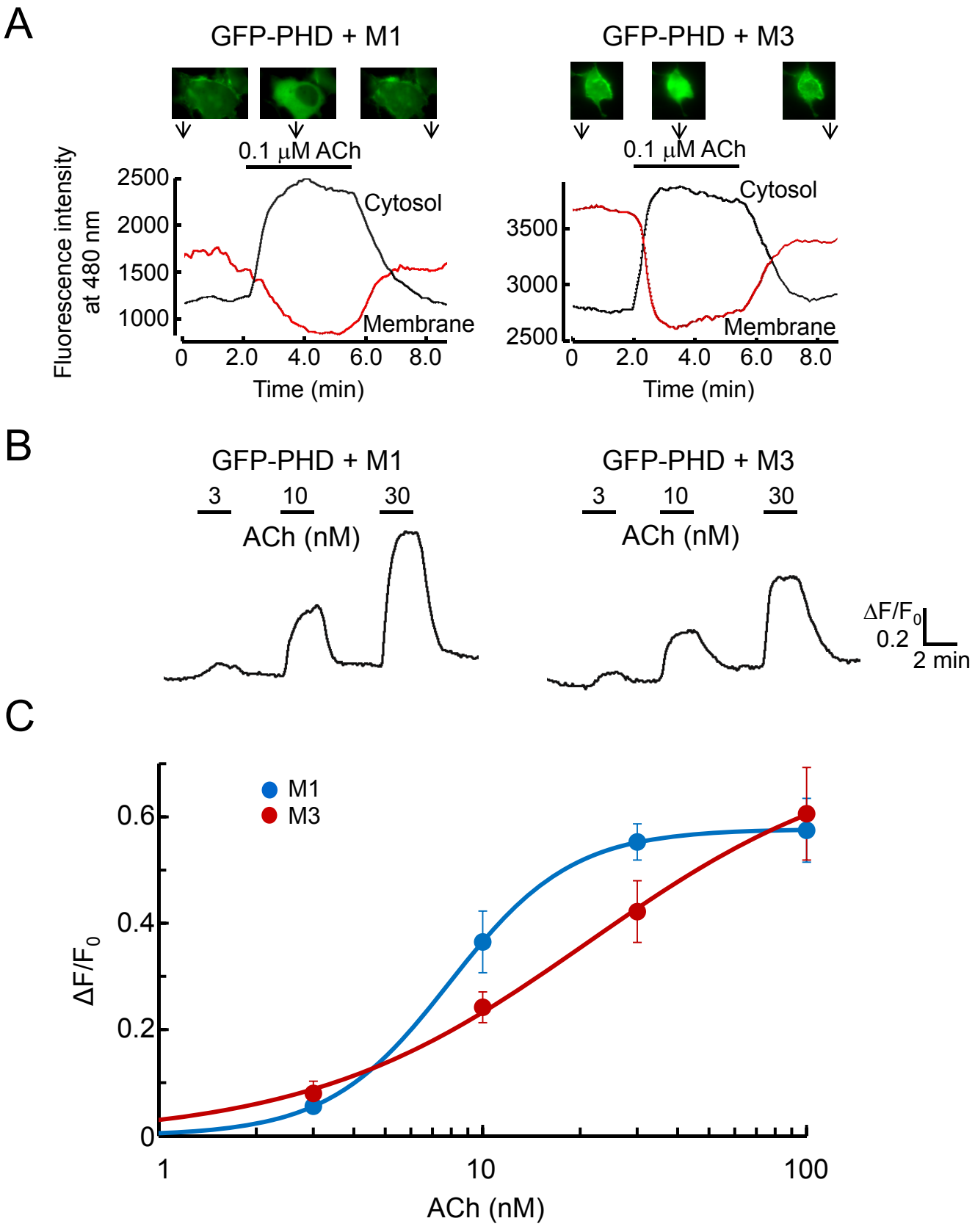
A
GFP-PHD + M1
GFP-PHD + M3
0.1 μM ACh
0.1 μM ACh
Fluorescence intensity at 480 nm
Cytosol
Membrane
Cytosol
Membrane
Time (min)
Time (min)
B
GFP-PHD + M1
GFP-PHD + M3
3
10
30
ACh (nM)
3
10
30
ACh (nM)
ΔF/F0
0.2
2 min
C
M1
M3
ΔF/F0
ACh (nM)

Fig. 4

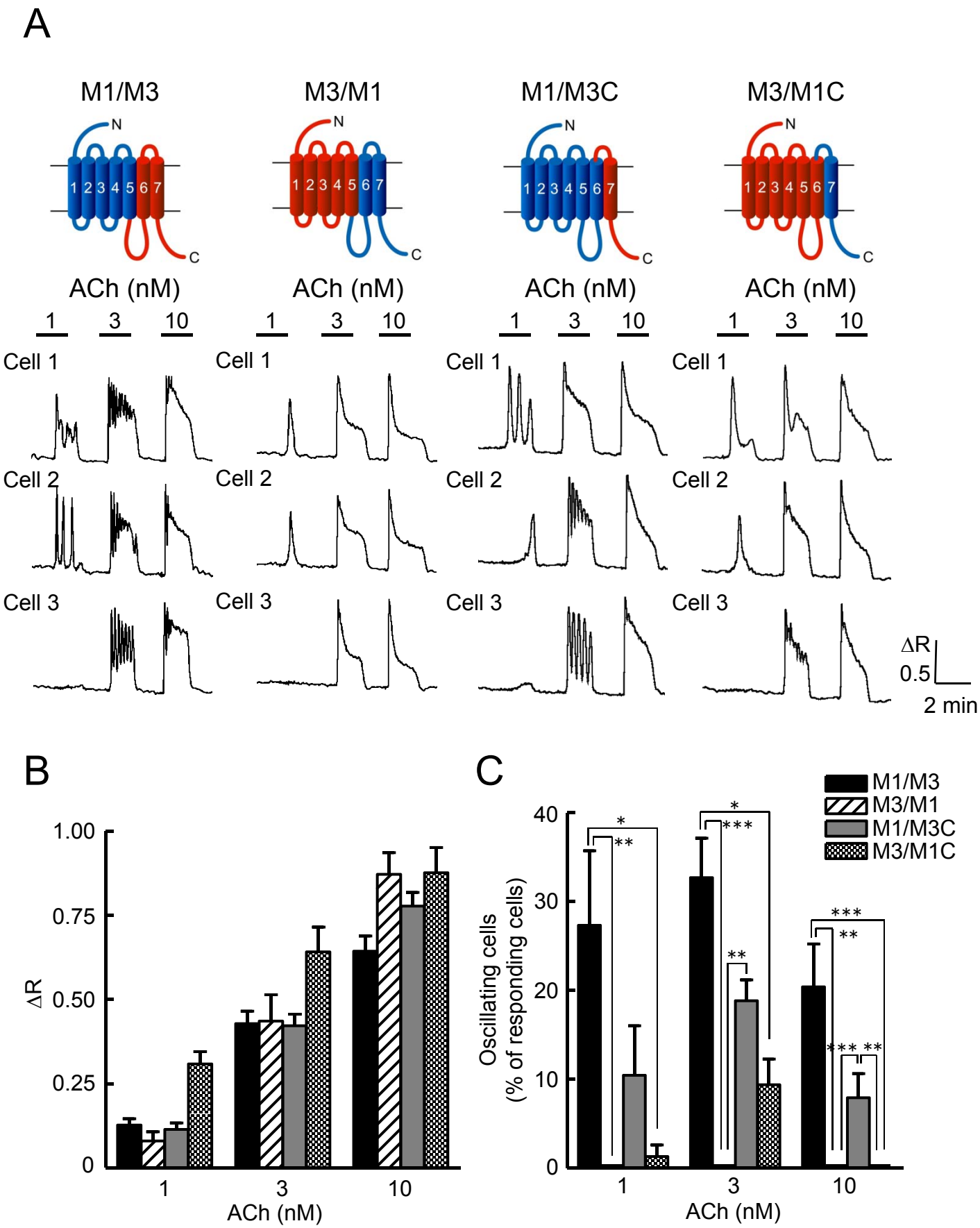
A
M1/M3
M3/M1
M1/M3C
M3/M1C
N
C
1 2 3 4 5 6 7
ACh (nM)
1
3
10
Cell 1
Cell 2
Cell 3
ΔR
0.5
2 min
B
1.00
0.75
0.50
0.25
0
ΔR
1
3
10
ACh (nM)
C
40
30
20
10
0
Oscillating cells
(% of responding cells)
M1/M3
M3/M1
M1/M3C
M3/M1C
*
**
***
1
3
10
ACh (nM)

Fig. 5

Supplementary Table 1: Primers for the construction of wild-type or chimeric mAChRs.

Gene	Orientation	Sequence
M1	Forward	TGGATCCGCCACCATGAACACTTCAGCCCCACC
	Reverse	CGAATTCTCAGCATTGGCGGGAGGGAG
M3	Forward	CGCTAGCCCACCATGACCTTGCACAATAACAG
	Reverse	CGAATTCCTACAAGGCCTGCTCGGGTG
M1/M3	Forward	CATCTACCGGGAGACTGAAAAGCGTACCAAAGAG
	Reverse	TACGCTTTTCAGTCTCCCGGTAGATGCGCCAGTAG
M3/M1	Forward	GATCTATAAGGAAACAGAGAACCGAGCACGGGAG
	Reverse	CTCGGTTCTCTGTTTCCTTATAGATCCTCCAG
M3/M1C	Forward	CAGACCCTCAGTGCCATCCTCCTGGCCTTCATCC
	Reverse	CAGGAGGATGGCACTGAGGGTCTGGGCCGCTTTC
M1/M3C	Forward	CGGACCCTGAGTGCGATCTTGCTTGCCTTCATC
	Reverse	AAGCAAGATCGCACTCAGGGTCCGAGCCGCC

The table lists the forward or reverse primer for M1, M3, M1/M3, M3/M1, M1/M3C and M3/M1C.

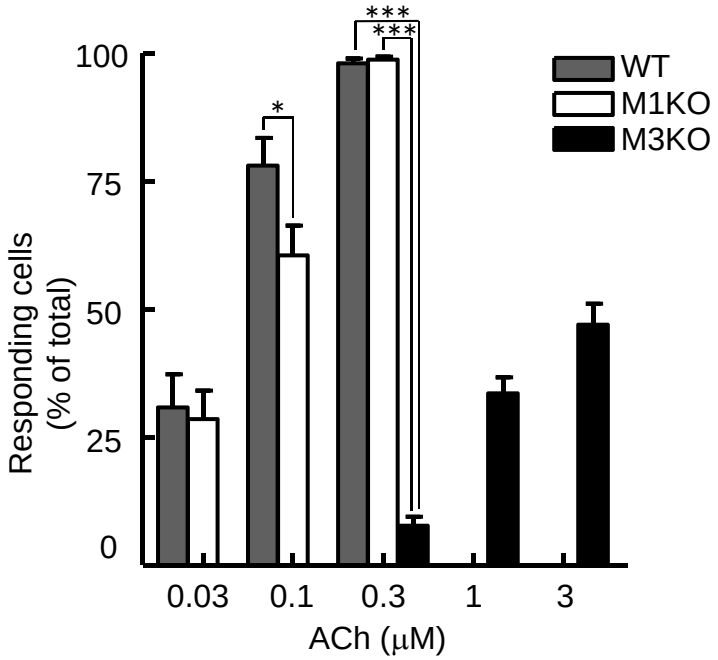

Supplementary Fig. S1. *The percentage of ACh-responding cells isolated from WT, M1KO and M3KO mice.*
Bar chart representing the number of responding cells isolated from WT, M1KO and M3KO (ACh 0.03, 0.1 and 0.3 μM in WT and M1KO; 0.3, 1 and 3 μM in M3KO). Statistical difference was assessed by Mann-Whitney U test. * $p < 0.05$, ** $p < 0.01$, *** $p < 0.001$.

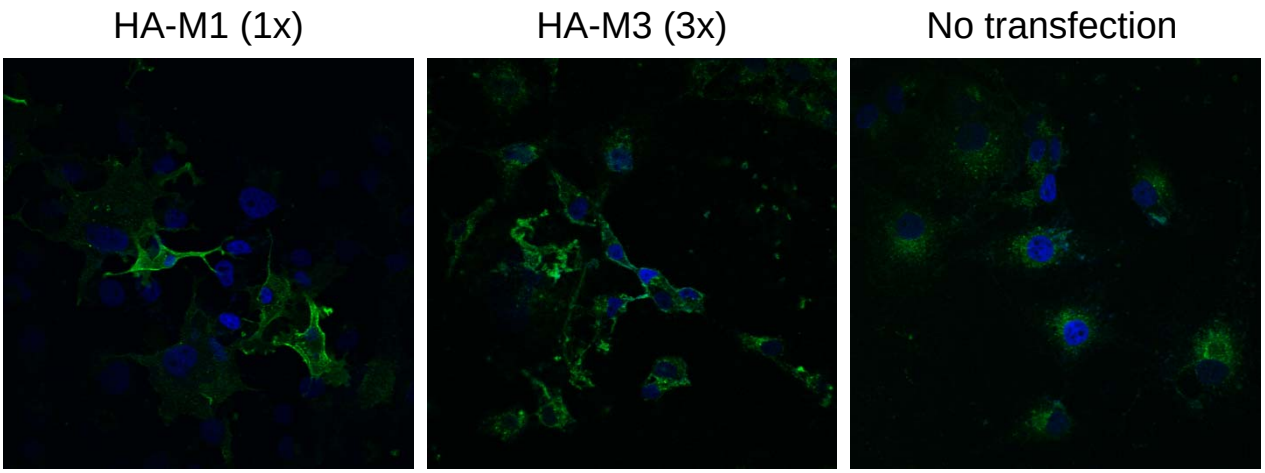

Supplementary Fig. S2. *Confocal images of HA-tagged M1 and M3 receptors transiently expressed in COS-7 cells.*
The fluorescence images of COS-7 cells transfected with HA-M1 or HA-M3, and of not transfected cells were observed under a confocal microscope with 60x oil immersion lens. Green, anti-HA immunostain. Blue, Hoechst 33342 stain.

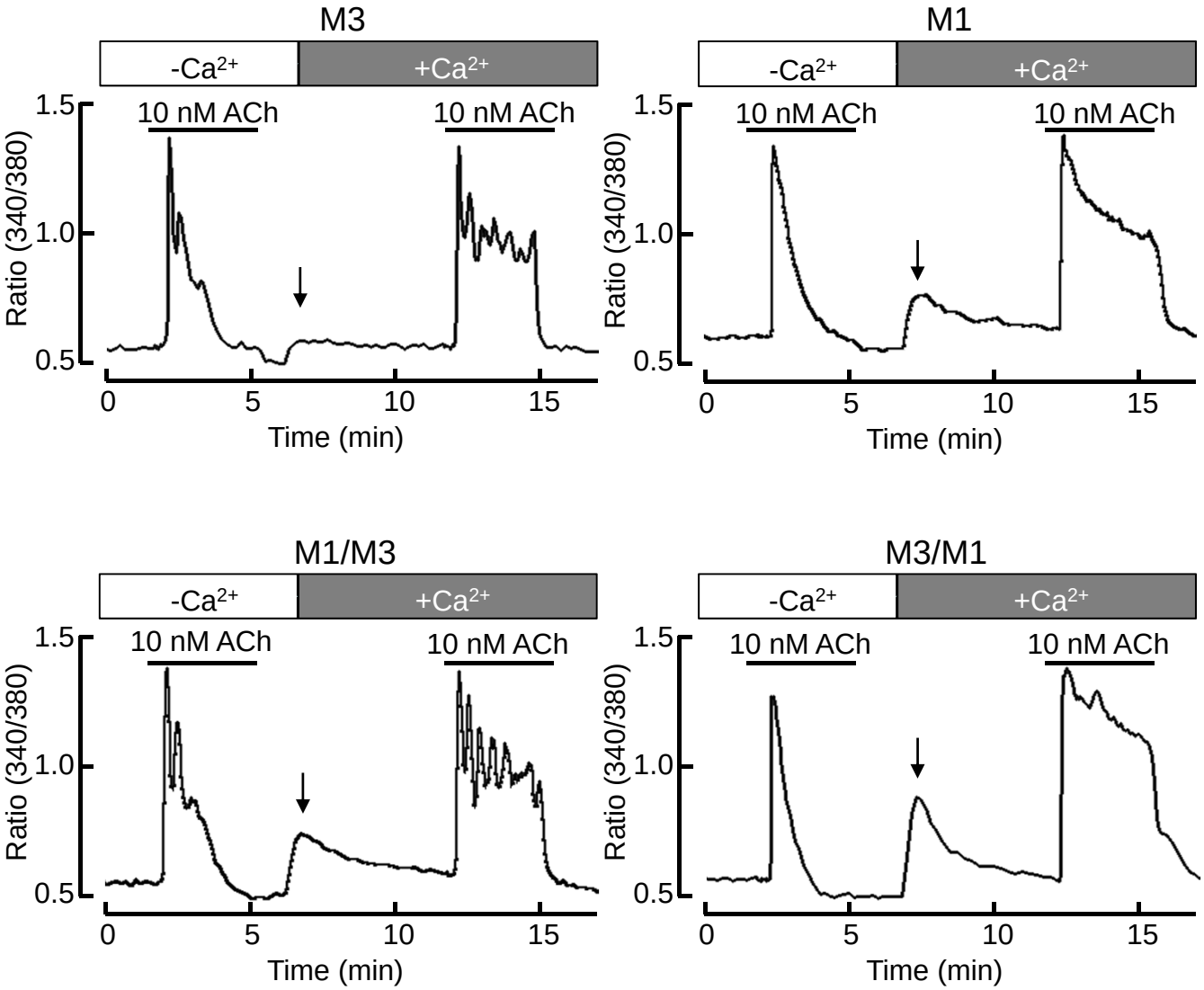

Supplementary Fig. S3. Comparison of ACh-induced Ca^{2+} dynamics in the absence or presence of extracellular Ca^{2+} .
Individual traces exhibit $[Ca^{2+}]_i$ response to ACh (10 nM) in COS-7 cells transfected with M3, M1, M1/M3, or M3/M1 receptors (total 8 - 45 responding cells from 2 - 5 experiments). Open or closed boxes indicate the perfusion of Ca^{2+}-free or Ca^{2+}-containing solutions, respectively. The arrow in each trace indicates the capacitive entry of Ca^{2+} which is observed when the external medium was exchanged from Ca^{2+}-free to normal BSS.

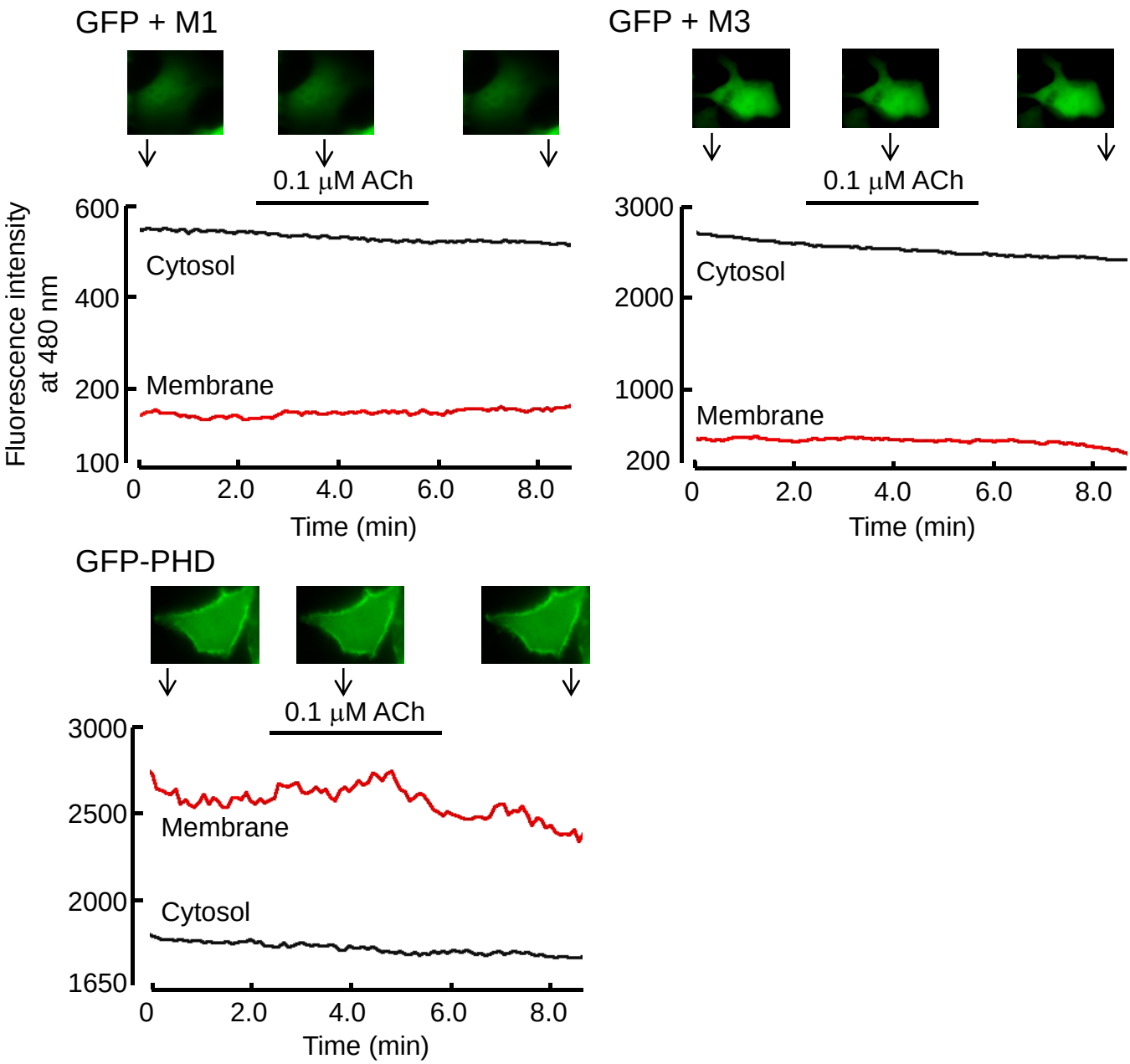

Supplementary Fig. S4. *The representative fluorescence responses in the two negative controls.*
The fluorescence changes at the cytoplasmic membrane (red) and cytosolic space (black) during the application of 0.1 μM ACh were acquired in COS-7 cells co-expressing EGFP and muscarinic receptors (upper panels). Reproducibility was confirmed by two independent experiments. We also confirmed the reproducibility of the lack of a response in EGFP-PHD-expressing COS-7 cells that were not transfected with muscarinic receptor plasmids in 4 independent experiments (lower panel).